

# Reconstruction of aerodynamic angles from flight data for “Slybird” Unmanned Aerial Vehicle (UAV)

Shikha Jain, Kamali C

*Scientist, Flight Mechanics and Control Division  
National Aerospace Laboratories  
Bangalore, India*

**Abstract**— The angle of attack and the sideslip angle are significant parameters describing the aerodynamics of the aircraft. Specifically, these angles are required for identification of the system parameters such as aerodynamic forces and moment derivatives. For exact measurements, it is necessary to install appropriate air data sensors on board. However, it is sometime difficult to install such apparatus on small UAVs. Inertial sensor measurements, aerodynamic derivatives and equations of motions are used to determine the aerodynamic angles. In this paper, three approaches are followed to estimate airflow angles. The first concept uses navigational equations for the estimation. In the second approach, inertial sensor data has been used. Third concept uses aerodynamic derivative obtained from wind tunnel testing. Estimated angles from all three approaches are shown for simulated and flight data. Complementary filter has been used for combining estimated angles obtained using inertial measurements and aerodynamic derivative based approaches. Improved filtered angles are compared with simulated airflow angles for the same flight condition.

## I. INTRODUCTION

The small size vehicles like UAVs and MAVs poses several stability and control challenges. The low damping ratio of these small vehicles causes large oscillations. Such vehicles tend to have high natural frequencies. They are also more susceptible to gusts because of their small size and low wing loading. To design robust control for these vehicles, knowledge on their stability and control derivatives is essential. They can be obtained from wind tunnel tests/CFD/empirical methods. But when the vehicle is flown, it could show different responses from what is predicted by the foregoing methods. Hence, these derivatives are estimated from the flight test data and the wind tunnel/CFD models are updated if there are any discrepancies. Accurate estimation of aircraft aerodynamic model parameters depends on angle of attack and sideslip angle. Instrumentation for air flow angles is much more difficult and expensive, both to install and to calibrate properly on small size vehicles. It would be advantageous if aerodynamic model parameters could be determined accurately from flight data without having to instrument the aircraft to measure air flow angles.

In this paper, three approaches are followed for reconstruction of aerodynamic angles. In the first approach, analytical method using equation of motions is used for deriving aerodynamic angles. The second method computes aerodynamic angles from inertial sensor measurements whereas in third method aerodynamic derivatives are used

along with accelerometer outputs. All the measurements used for reconstruction are corrupted by different types of spectral noise to simulate the realistic conditions. To overcome the effect of noisy data, angles computed using inertial sensor and aerodynamic derivatives based approaches are combined using complementary filter. Complementary filter combines two independent noisy measurements having different spectral noise of a same signal. This leads to an improved approach for determining the aerodynamics angles.

For the performance evaluation of all the techniques, Slybird flight and simulation data is used. Slybird is a mini Unmanned Aerial Vehicle (UAV), shown in figure 1, developed by the National Aerospace Laboratories (NAL) with a primary intention of surveillance [1]. A complete 6DOF simulation model is developed in Matlab/Simulink platform using non linear look tables obtained from low speed wind tunnel tests. Its onboard sensor and aerodynamic data obtained from wind tunnel tests is used. The primary users of this bird will be police and military services. It is a hand launched with soft landing capability. It has an endurance of one hour with a range of 10 km.



Figure 1. NAL-“Slybird”

The paper is organized as follows: Section II covers the modeling for the estimation of flow angles. Section III gives brief introduction about 6DOF simulation model. Results using simulation and flight data is presented in section IV followed by conclusions in last section.

## II. ESTIMATION OF FLOW ANGLES

Flight Vehicle aerodynamics strongly depend on airflow angles, namely Angle Of Attack (AOA ( $\alpha$ )) and Angle of Sideslip (AOSS ( $\beta$ )). In this Section, three approaches for

estimation have been discussed. The first approach uses navigational equations of aircraft for deriving aerodynamic angles.

#### A. Using Kinematic/Navigational Equations

The navigational equations in terms velocity of the UAV ( $u, v, w$ ) with respect to the inertial velocity components expressed in the body frame can be written as (1).

Assuming a low wind conditions, body axes velocity components can be written in terms of airspeed ( $V_T$ ), angle of attack ( $\alpha$ ) and sideslip angle ( $\beta$ ) as

$$\begin{aligned} u &\approx V_T \cos \alpha \cos \beta \\ v &\approx V_T \sin \beta \\ w &\approx V_T \sin \alpha \cos \beta \end{aligned} \quad (2)$$

The navigation equation can be written in terms of  $V_T$ ,  $\alpha$  and  $\beta$  by substituting (2) into (1) as (3)

Further  $\frac{\dot{y}}{\dot{x}} = \tan \Gamma$ ; where  $\Gamma$  is a track angle and equal to right hand side of (4).  $\dot{h}$  can be further rewritten as

$$\frac{\dot{h}}{V_T} = \cos \alpha \cos \beta \sin \theta - \cos \theta (\sin \beta \sin \phi + \sin \alpha \cos \beta \cos \phi) \quad (5)$$

Rearranging the (5) as

$$\frac{\frac{\dot{h}}{V_T} + \sin \beta \sin \phi \cos \theta}{\cos \beta} = (\cos \alpha \sin \theta - \sin \alpha \cos \phi \cos \theta) \quad (6)$$

By defining  $\sin \Theta = \frac{\sin \theta}{D}$ ;  $\cos \Theta = \frac{\cos \theta \cos \phi}{D}$

and  $D = \sin^2 \theta + \cos^2 \theta \cos^2 \phi$ , right hand side of (6) can be written as

$$\begin{aligned} \frac{\frac{\dot{h}}{V_T} + \sin \beta \sin \phi \cos \theta}{D \cos \beta} &= \cos \alpha \sin \Theta - \sin \alpha \cos \Theta \\ &= \sin(\Theta - \alpha) \end{aligned} \quad (7)$$

Similarly, by defining

$$\begin{aligned} A &= \Upsilon \cos \Phi \\ &= \cos \alpha \cos \beta \cos \theta + (\sin \beta \sin \phi + \sin \alpha \cos \beta \cos \phi) \sin \theta \\ B &= \Upsilon \sin \Phi = \sin \beta \cos \phi - \sin \alpha \cos \beta \sin \phi \end{aligned}$$

$$\text{and } \Upsilon = \sqrt{A^2 + B^2},$$

Substituting  $A, B$  and  $\Upsilon$  into right hand side of equation (4), it can be written as  $\tan(\psi + \Phi)$  by using trigonometry expression.

$$\frac{\dot{y}}{\dot{x}} = \tan \Gamma, \quad \frac{\Upsilon \cos \Phi \sin \psi + \Upsilon \sin \Phi \cos \psi}{\Upsilon \cos \Phi \cos \psi - \Upsilon \sin \Phi \sin \psi} = \tan(\psi + \Phi) \quad (8)$$

Then,  $\Gamma = \psi + \Phi$

and

$$\Phi = \Gamma - \psi = \tan^{-1} \left( \frac{B}{A} \right) \quad (9)$$

$$\tan(\Gamma - \psi) = \frac{\sin \beta \cos \phi - \sin \alpha \cos \beta \sin \phi}{\cos \alpha \cos \beta \cos \theta + (\sin \beta \sin \phi + \sin \alpha \cos \beta \cos \phi) \sin \theta} \quad (10)$$

Further, equation (10) can be rewritten as following

$$\tan(\Gamma - \psi) = \frac{\tan \beta \cos \phi - \sin \alpha \sin \phi}{\cos \alpha \cos \theta + (\tan \beta \sin \phi + \sin \alpha \cos \phi) \sin \theta} \quad (11)$$

---


$$\begin{aligned} \dot{x} &= (u \cos \theta + (v \sin \phi + w \cos \phi) \sin \theta) \cos \psi - (v \cos \phi - w \sin \phi) \sin \psi \\ \dot{y} &= (u \cos \theta + (v \sin \phi + w \cos \phi) \sin \theta) \sin \psi + (v \cos \phi - w \sin \phi) \cos \psi \\ \dot{h} &= u \sin \theta - (v \sin \phi + w \cos \phi) \cos \theta \end{aligned} \quad (1)$$

$$\begin{aligned} \dot{x} &= V_T [(\cos \alpha \cos \beta \cos \theta + \sin \beta \sin \phi \sin \theta + \sin \alpha \cos \beta \cos \phi \sin \theta) \cos \psi - (\sin \beta \cos \phi - \sin \alpha \cos \beta \sin \phi) \sin \psi] \\ \dot{y} &= V_T [(\cos \alpha \cos \beta \cos \theta + \sin \beta \sin \phi \sin \theta + \sin \alpha \cos \beta \cos \phi \sin \theta) \sin \psi + (\sin \beta \cos \phi - \sin \alpha \cos \beta \sin \phi) \cos \psi] \\ \dot{h} &= V_T \cos \alpha \cos \beta \sin \theta - (V_T \sin \beta \sin \phi + V_T \sin \alpha \cos \beta \cos \phi) \cos \theta \end{aligned} \quad (3)$$

$$\frac{\dot{y}}{\dot{x}} = \frac{(\cos \alpha \cos \beta \cos \theta + \sin \beta \sin \phi \sin \theta + \sin \alpha \cos \beta \cos \phi \sin \theta) \sin \psi + (\sin \beta \cos \phi - \sin \alpha \cos \beta \sin \phi) \cos \psi}{(\cos \alpha \cos \beta \cos \theta + \sin \beta \sin \phi \sin \theta + \sin \alpha \cos \beta \cos \phi \sin \theta) \cos \psi - (\sin \beta \cos \phi - \sin \alpha \cos \beta \sin \phi) \sin \psi} \quad (4)$$


---

Angle of attack  $\alpha$  and sideslip angle  $\beta$  is derived from (7) and (11) respectively as

$$\alpha = \sin^{-1} \left[ \frac{\sin \theta}{\mathbf{D}} \right] - \sin^{-1} \left[ \frac{\frac{\dot{h}}{\mathbf{V}_T} + \sin \beta \sin \phi \cos \theta}{\mathbf{D} \cos \beta} \right]$$

Trim conditions for a steady, straight and level flight at low angle of attack, in low wind conditions are

$$\beta = p = q = r = \phi = 0 \text{ and } \alpha = \theta$$

Using these conditions, further  $\alpha$  can be written as

$$\alpha = \sin^{-1} \left[ \frac{\sin \theta}{\mathbf{D}} \right] - \sin^{-1} \left[ \frac{\frac{\dot{h}}{\mathbf{V}_T * \mathbf{D}}}{\mathbf{V}_T * \mathbf{D}} \right] \quad (12)$$

and

$$\beta = \tan^{-1} \left( \frac{\tan(\Gamma - \psi)(\cos \alpha \cos \theta + \sin \alpha \cos \phi \sin \theta) + \sin \alpha \sin \phi}{\cos \phi - \sin \phi \sin \theta \tan(\Gamma - \psi)} \right) \quad (13)$$

$\dot{h} = -V_d$  is obtained from GPS measurement whereas  $\mathbf{V}_T$  is obtained using onboard pressure sensor measurement. Attitudes angles are obtained from Extended Kalman Filter based INS/GPS integration. A 16 state filter is implemented which estimate positions, velocities, 4 quaternions and biases for gyro and accelerometers. This method is very sensitive with respect to the accuracy of the sensor data.

### B. Using Inertial Measurements

The second method uses the inertial data, namely the angular rates  $p$ ,  $q$ , and  $r$ , and the translational accelerometer measurements  $a_x$ ,  $a_y$  and  $a_z$ , for reconstruction of alpha and beta angle. The translational equations of motion for a rigid aircraft in body axes are

$$\dot{u} = rv - qw + \frac{\bar{q}SC_x}{m} - g \sin \theta + \frac{T_x}{m} \quad (14)$$

$$\dot{v} = pw - ru + \frac{\bar{q}SC_y}{m} + g \cos \theta \sin \phi \quad (15)$$

$$\dot{w} = qu - pv + \frac{\bar{q}SC_z}{m} + g \cos \theta \cos \phi + \frac{T_z}{m} \quad (16)$$

This method is implemented assuming small angle approximation for  $\alpha$  and  $\beta$  during a steady state flight conditions. For these conditions, the body axis accelerometers approximately measure the thrust and aerodynamic forces [4]. Further, replacing acceleration measurements for the applied forces results in the translational kinematic equations in body axes as

$$\dot{u} = rv - qw - g \sin \theta + a_x \quad (17)$$

$$\dot{v} = pw - ru + g \cos \theta \sin \phi + a_y \quad (18)$$

$$\dot{w} = qu - pv + g \cos \theta \cos \phi + a_z \quad (19)$$

Typically, small perturbation maneuvers are performed during the flights testing for aerodynamic parameter estimation. The perturbation is about a reference condition of steady, straight-and-level flight at nominal angle of attack, in calm conditions. With these assumptions, the following approximations hold good [5]:

$$u \approx \mathbf{V}_T \approx \text{constant} \quad (20)$$

$$\beta \approx \frac{v}{\mathbf{V}_T} \quad (21)$$

$$\alpha \approx \frac{w}{\mathbf{V}_T} \quad (22)$$

Combining above equations from (17) to (22) and trim conditions given in subsection A of section II, derivative of aerodynamic angles can be written as

$$\dot{\alpha} = \frac{g \cos \theta \cos \phi + a_z}{\mathbf{V}_T} + q \quad (23)$$

$$\dot{\beta} = \frac{g \cos \theta \sin \phi + a_y}{\mathbf{V}_T} - r \quad (24)$$

Equation (23) and (24) holds good for mild turbulence profile [6]. Inertial data used in this technique is corrected for bias using INS/GPS integration filter. The limitation with this approach is that the measured values for the inertial data are prone to bias errors. This technique causes a time-dependent drift in the  $\beta$  and  $\alpha$  reconstructions, even for small bias errors. This is due to, the additive effect of the time integration. Hence, to overcome this, a high pass filter is applied to remove the low frequency noise present in rate measurements.

### C. Using Aerodynamic Derivatives

In this approach, based on the knowledge of nondimensional stability and control derivatives obtained from wind tunnel/CFD tests and inertial data, aerodynamic angles are obtained using following relations [3, 4].

$$\alpha = \frac{1}{C_{L_\alpha}} \left( \frac{m}{\bar{q}S} a_z - C_{L_0} - C_{L_{\delta e}} \delta e - \frac{\bar{c}q}{2V_T} C_{L_q} \right) \quad (25)$$

$$\beta = -\frac{1}{C_{Y_\beta}} \left( \frac{m}{\bar{q}S} a_y + C_{Y_{\delta r}} \delta r + \frac{b}{2V_T} (C_{Y_p} p + C_{Y_r} r) \right) \quad (26)$$

In this work, aerodynamic coefficients are obtained from low speed wind tunnel tests carried out at HAL [1]. In order to suppress high frequency noise in accelerometer measurements, a low pass filtering is applied. This class of vehicles won't be flying at very high angle of attack and usually developed for surveillance purpose. A 6dof simulation for Slybird has been developed and validated against flight data [2]. Therefore, aerodynamic coefficients obtained wind tunnel test can be used in this approach and approximated relations holds good for steady and calm conditions.

#### D. Complementary filter approach

Approaches discussed under subsections B and C could be independently used. But they are not very accurate due to low frequency bias errors and high frequency noise. Hence, to obtain a better reconstruction of flow angles, estimated angles obtained from above two techniques (Equation (23) & (25) for AOA and Equation (24) & (26) for AOSS) are combined by using complementary filter [3, 4]. It seems to improve the overall system bandwidth. Fig. 2, shows a direct complementary filter that uses two measurements to obtain an estimate of aerodynamic angles.

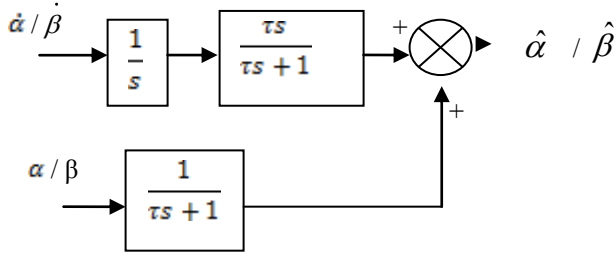


Fig. 2. A direct complementary filter

In the following section, results from all the techniques and filtered aerodynamic angles are presented.

#### III. 6DOF SIMULATION MODEL FOR SLYBIRD

To compare the performance of all the three approaches, a reference is required. Airflow sensors are not available on the aircraft to get the measurement for reference angles. Therefore, simulated flow angles responses from Slybird 6DOF model is considered as reference. Simulation model should be validated before using its responses for reference purpose.

**Simulation model:** A complete 6-DOF nonlinear model for the UAV is built in the Matlab/Simulink environment considering forces and moments due to aerodynamics and

propeller/engine to simulate realistic dynamic behaviour of the aircraft. The standard 6DOF equations of motion (i.e., flat earth approximation)) for a fixed wing aircraft are used. Traditionally, the nondimensional coefficients for the aerodynamic forces and moments are approximated by a linear sum of contributing parameters utilizing the stability and control derivatives in a specified flight condition. Precise knowledge of such derivatives is essential towards the development of a high fidelity simulation.

Building a simulation model for a 6DOF model requires the following data:

- Aerodynamic data
- Propulsion data
- Mass, centre of gravity, inertia and moment reference point data
- Geometry data such as wing-span, mean aerodynamic chord and wing surface area.

Wind tunnel test can be utilized to obtain these derivatives experimentally. 1:1 scale Slybird model was tested at HAL low speed wind tunnel in order to determine the aerodynamic characteristic [1]. The development of 6DOF simulation model has carried out on the basis of data obtained from non linear look tables constructed using low speed wind tunnel tests data. The aerodynamic model is implemented as per the application rules formulated in [1]. Simulink model is shown in fig. 3.

The Simulink program is capable of accepting trim conditions and control inputs i.e. elevator, aileron, rudder, and throttle. This allows the user to input the identical control surface deflections that were input during actual flight test. To validate the accuracy of the simulation, its responses are compared with flight test data.

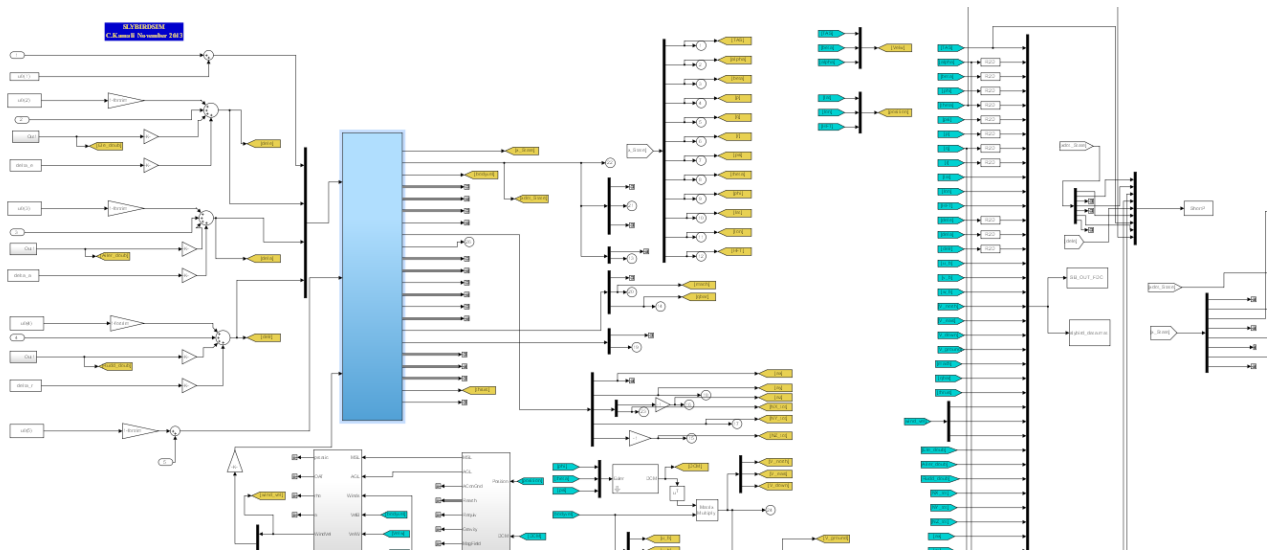


Figure 3. 6DOF Simulation model of Slybird

#### IV. RESULTS & ANALYSIS

The aircraft is test flown and the flight data is recorded. Flight test data were collected during maneuvers initiated from a trim condition of steady and straight level flight by exciting each control surface. Flight testing activities are conducted at Hoskote (approx 27 km from NAL). The experimental segment includes approximately 4-5 individual segments of straight and level flight, each lasting about 10s, flown at an average altitude of 920 m Above Mean Sea Level (AMSL) at an average airspeed of 18 m/s, during which traditional doublet maneuvers are injected manually by the R/C pilot. Specifically, elevator doublets were injected by the pilot for exciting the longitudinal dynamics while aileron doublets and rudder/aileron doublet combinations were used for exciting the lateral-directional dynamics. The sensor measurements were sampled at 50 Hz. The recorded data comprises of measurements from gyro, accelerometer, GPS, pressure sensor and air speed sensor.

##### A. 6DOF Model Validation

To test and validate the model against real flights, the response of the real aircraft is compared to the response of the software model when the same input parameters are applied. This allows the simulation model to be changed or fine tuned as required to prepare for reliable testing. From the entire set of flight data, short segments representing the longitudinal and lateral directional maneuvers were extracted for validating the model. The results of the actual flights in comparison with the Matlab/SIMULINK simulation of flight model for longitudinal and lateral dynamics are given in figure 4 & 5 respectively.

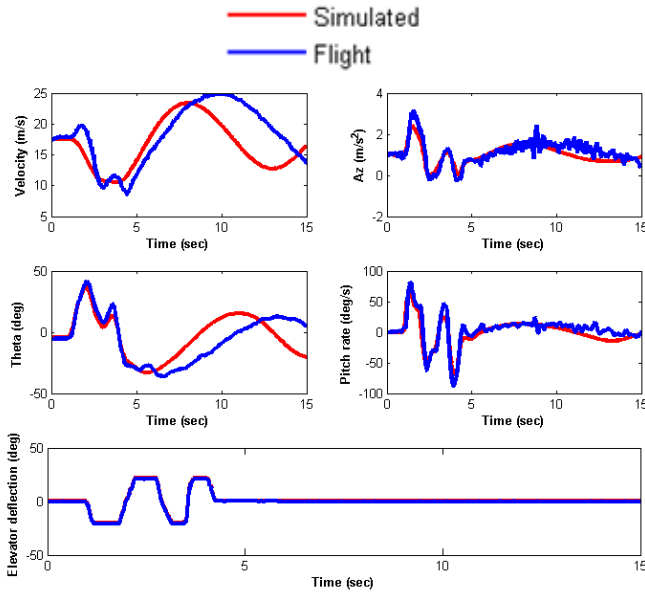


Figure 4. Longitudinal Dynamics - Flight vs. Simulated Output

Real flight data matches well with simulation responses. Therefore, aerodynamic angles generated by the simulation model for the given input can be used as reference for comparison of approaches given in section II.

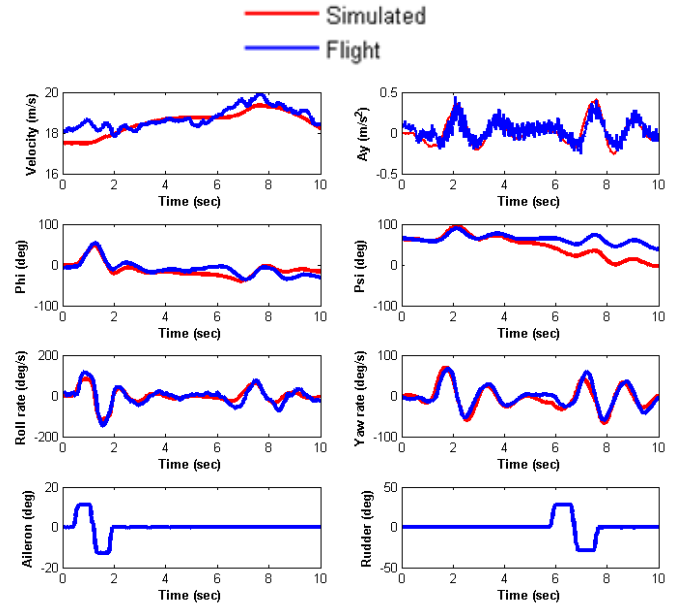


Figure 5. Lateral Directional Dynamics- Flight vs. Simulated Output

##### B. Aerodynamic angles Reconstruction

The performance of all the techniques is evaluated using simulated and flight data. The results are shown by comparing the aerodynamic angles with their corresponding true angles. Simulated responses are taken as true/reference angles.

###### B.1 Angle of attack ( $\alpha$ ) estimation

Angle of attack is computed using equation (12), (23) and (25). Fig. 6 shows the result for simulated data.

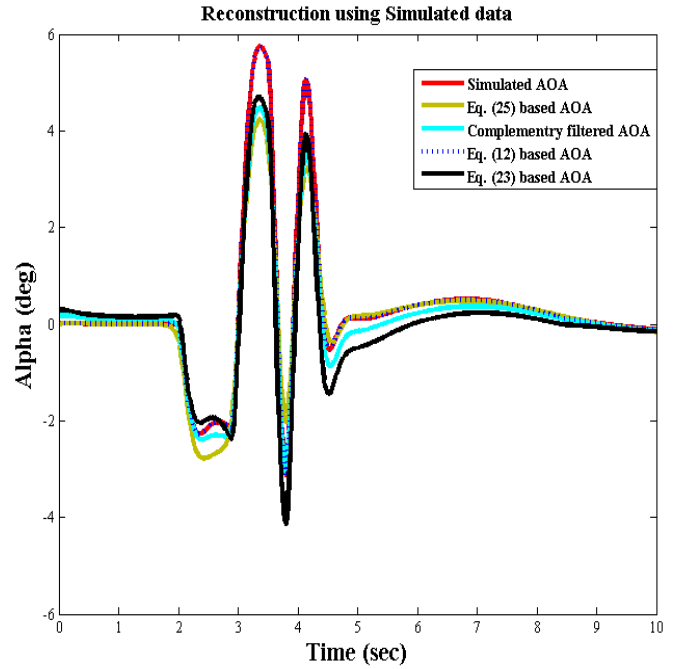


Fig. 6. Reconstruction of angle of attack from simulated data

To analyze further, techniques are tested for real data. Flight data responses are shown in Fig. 7. The segment of flight data, each with an approximate duration of 10s, encompassing the elevator doublet maneuver was given as a

canned input to the nonlinear 6DOF simulation model. Simulated angle of attack is compared with reconstructed angle from flight data.

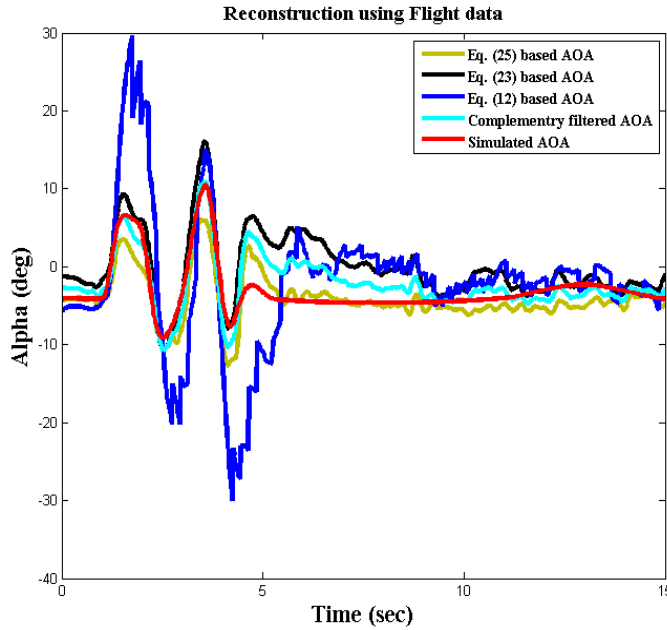


Fig. 7. Reconstruction of angle of attack from flight data

## B.2 Sideslip angle estimation

Sideslip angle is computed using equation (13), (24) and (26). The segments of rudder deflection, encompassing the doublet maneuver was fed into nonlinear 6DOF model. Fig. 8, presents a comparison of estimation results obtained with simulated data. Flight data results are shown in Fig. 9.

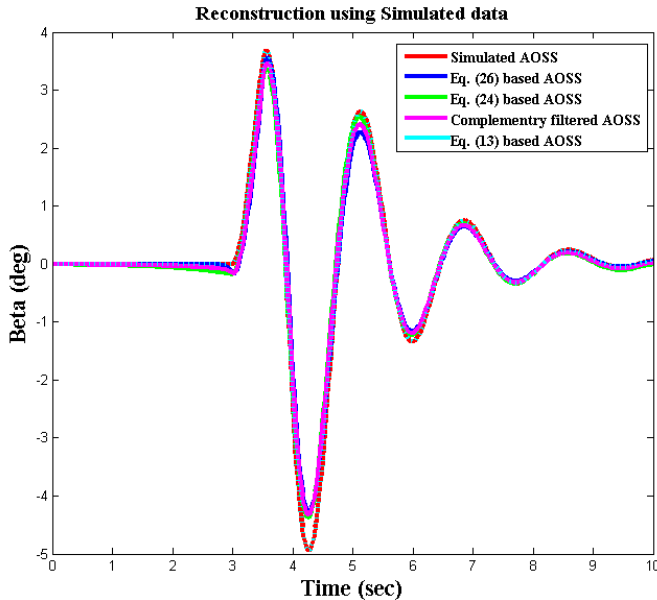


Fig. 8. Reconstruction of sideslip angle from simulated data

It has been observed that aerodynamic angles reconstructed using simulated data matches well with nonlinear 6 DOF time responses with respect to all the approaches. However, while testing with flight data, reconstruction using navigational equations is very sensitive to noisy data and could not produce accurate reconstruction

whereas complementary filtering based computations are closer to the simulated responses of the aerodynamic angles.

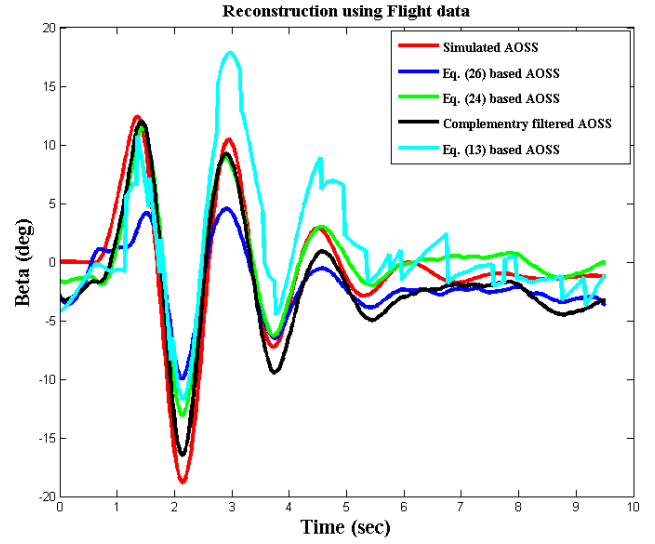


Fig. 9. Reconstruction of sideslip angle from flight data

## V. CONCLUSION

Various approaches for the reconstruction of aerodynamic angles using simulated and flight data are presented. Simulated aerodynamic angles obtained from Slybird nonlinear 6DOF model is used as true/ reference. All the techniques worked satisfactorily for simulated data. However for flight data, it has been observed that aerodynamic angles (angle of attack & sideslip angle) computed using complementary filtering, by combining two concepts, are more close to the simulated responses of aerodynamic angles. In future, these techniques will be applied for flow angle computations and parameter identification will be carried out using the same.

## REFERENCES

- [1] C Kamali, Alexander Kale, "Development of Six DOF model for Class-I MAV", technical report, NAL, September, 2013.
- [2] Shikha Jain, C Kamali, "Simulation, Experimental validation of 6DOF slybird simulation model using flight data", technical report, NAL, December 2013.
- [3] M. Heller, S. Myszchik et al, "Low cost approach based on navigation data for determining angles of attack and sideslip for small aircraft", AIAA Guidance, Navigation and Control Conference and Exhibit, August 2003.
- [4] D. Jung and P. Tsiotras, "Modeling and Hardware in the loop simulation for a small unmanned aerial vehicle", AIAA 2007.
- [5] Eugene A. Morelli, "Real-Time Aerodynamic Parameter Estimation without Air Flow Angle Measurements", AIAA 2010.D.
- [6] C Kamali, A A Pashilkar, J R Raol, "Evaluation of recursive least square algorithm for parameter estimation in aircraft real time applications", Aerospace science and technology, vol. 15, May 2011.